Bone Reports 11 (2019) 100224

Contents lists available at ScienceDirect

Bone Reports

journal homepage: www.elsevier.com/locate/bonr

Effect of alendronate or 8-prenylnaringenin applied as a single therapy or in combination with vibration on muscle structure and bone healing in ovariectomized rats

M. Komrakova[a,*], C. Rechholtz[a], N. Pohlmann[a], W. Lehmann[a], A.F. Schilling[a], R. Wigger[b], S. Sehmisch[a,1], D.B. Hoffmann[a,1]

[a] Department of Trauma Surgery, Orthopaedics and Plastic Surgery, University Medical Center Goettingen, Robert-Koch Str. 40, 37075 Goettingen, Germany
[b] Department of Animal Sciences, University of Goettingen, Albrecht-Thaer-Weg 3, 37075 Goettingen, Germany

ARTICLE INFO

Keywords:
Bisphosphonate alendronate
Phytohormone 8-prenylnaringenin
Vibration
Osteoporosis
Bone healing
Muscle

ABSTRACT

Bisphosphonate alendronate (ALN), phytoestrogen 8-prenylnaringenin (8-PN) and the whole body vibration exert a favorable effect on osteoporotic bone. However, the impact of these treatments and the combination of pharmacological therapies with biomechanical stimulation on muscle and bone has not yet been explored in detail. The effect of ALN and 8-PN and their combination with the vibration (Vib) on skeletal muscle and bone healing was investigated in ovariectomized (Ovx) rats.

Three-month old rats were Ovx (n = 78), or left intact (Non-Ovx; n = 12). Five weeks after Ovx, all rats were treated according to the group assignment (n = 12/13): 1) Non-Ovx; 2) Ovx; 3) Ovx + Vib; 4) Ovx + ALN; 5) Ovx + ALN + Vib; 6): Ovx + 8-PN; 7) Ovx + 8-PN + Vib. Treatments with ALN (0.58 mg/kg BW, in food), 8-PN (1.77 mg/kg BW, daily s.c. injections) and/or with vertical vibration (0.5 mm, 35 Hz, 1 g, 15 min, 2×/day, 5×/week) were conducted for ten weeks. Nine weeks after Ovx, all rats underwent bilateral tibia osteotomy with plate osteosynthesis and were sacrificed six weeks later.

Vibration increased fiber size and capillary density in muscle, enlarged callus area and width, and decreased callus density in tibia, and elevated alkaline phosphatase in serum. ALN and ALN + Vib enhanced capillarization and lactate dehydrogenase activity in muscle. In tibia, ALN slowed bone healing, ALN + Vib increased callus width and density, enhanced callus formation rate and expression of osteogenic genes. 8-PN and 8-PN + Vib decreased fiber size and increased capillary density in muscle; callus density and cortical width were reduced in tibia. Vibration worsened 8-PN effect on bone healing decreasing the callus width and area.

Our data suggest that Vib, ALN, 8-PN, or 8-PN + Vib do not appear to aid bone healing. ALN + Vib improved bone healing; however application is questionable since single treatments impaired bone healing. Muscle responds to the anti-osteoporosis treatments and should be included in the evaluation of the drugs.

1. Introduction

Osteoporosis is a bone disease characterized by the deterioration of bone structure with a consequent increase in bone fragility (Turner et al., 1994; Hernlund et al., 2013; Frost, 1997). The factors that affect the bone may also influence the muscle tissue (Burr, 1997; Rolland et al., 2008). Age-related reductions in bone strength are preceded by deterioration in muscle strength (Frost, 1997; Burr, 1997; Rolland et al., 2008). The role of muscle in the development of osteoporosis remains unclear (Wolfe, 2006); however, bone fractures can be efficiently prevented by assessment of muscle strength and consequential inclusion of at-risk patients in fall-prevention programs (Hsu et al., 2014). The impact of most anti-osteoporosis treatments on the muscle has not yet been explored in detail.

The reduction in the bone mass of osteoporotic patients is most commonly treated using bisphosphonates. Bisphosphonates inhibit osteoclast activity, thereby reducing bone resorption and consequently improving bone mineral density (Orwoll et al., 2000). Few studies have investigated the effect of bisphosphonates on muscle tissue. Widrick et al. (2007) stated that alendronate (ALN) had no effect on muscle contractility. Uchiyama et al. (2015) observed a reduced muscle cross sectional area in long-term bisphosphonate users compared with

* Corresponding author.
E-mail address: marina.komrakova@med.uni-goettingen.de (M. Komrakova).
[1] Sehmisch and Hoffmann equally contributed to this study.

https://doi.org/10.1016/j.bonr.2019.100224
Received 18 December 2018; Received in revised form 19 August 2019; Accepted 26 August 2019
Available online 27 August 2019

controls.

The decline in muscle mass with age is correlated with a decline in estrogen level. Further, estrogen exerts a positive effect on muscle through the estrogen receptor (ER) α receptor (Collins et al., 2018). Consequently, hormone replacement therapy (HRT) was previously used as an efficient treatment against muscle loss and osteoporosis. However, there are considerable overall health risks associated with this treatment that outweigh its benefits in most cases (Anderson et al., 2004; Gambacciani and Levancini, 2014).

Phytoestrogens may be an alternative to HRT (Luo et al., 2014). Specifically, 8-prenylnaringenin (8-PN) is one of the most potent phytoestrogens known to date with a high affinity for ERα (Milligan et al., 2002; Keiler et al., 2013). 8-PN is found in hops (*Humulus lupulus* L.) and beer. Hops dietary supplements are used by women for *postmenopausal* symptom relief. 8-PN exerts favorable effects on osteoporotic bone properties and atrophied muscle tissue (Sehmisch et al., 2008; Mukai et al., 2012), with less effects on the uterus and endometrium (Hümpel et al., 2005a).

Whole body vibration (Vib) positively influences muscle and bone tissues and is considered as alternative treatment of muscle loss and osteoporosis (Bosco et al., 1999; Slatkovska et al., 2010). In postmenopausal women, vibrations (35–40 Hz, 2–5 *g*) increased hip bone mineral density and improved muscle strength (Verschueren et al., 2004). Different vibration regimes have been used in experimental studies, and vertical vibration of low magnitude and high frequencies (17–50 Hz, 0.3–3 *g* acceleration) are reportedly most effective in muscle and osteoporotic bone of rats (Chow et al., 2011; Oxlund et al., 2003; Rubinacci et al., 2008; Komrakova et al., 2013). The International Organization for Standardization (ISO) defined high-intensity vibrations (those that produce force > 1 *g*) as hazardous for human beings (ISO, 1997; Wysocki et al., 2011).

Recently, it was shown that vibration increased the favorable effect of alendronate, estrogen, and raloxifene (Chen et al., 2014; Stuermer et al., 2014; Wehrle et al., 2015a); however, it had no effect in combination with the strontium ranelate (SR) or 8-PN on osteoporotic bone tissue (Hoffmann et al., 2016a 2016b). The combined therapy of vibration with parathyroid hormone (PTH) applied at doses of 10 or 40 μg/kg BW did not show any synergetic effect on bone tissue (Lynch et al., 2011; Campos et al., 2018), whereas bone anabolic effect of PTH at lower dose (5 μg/kg BW) was enhanced by the vibration treatments (Campos et al., 2018). A favorable effect of vibration was observed on muscle structure when vibration was applied in combination with anti-osteoporosis drugs, such as teriparatide (PTH) and strontium ranelate (SR) (Komrakova et al., 2016).

The present investigation extends these studies, attempting to explore the effect of ALN and 8-PN as well as their combination with vibration on skeletal muscle in ovariectomized (Ovx) rats. Furthermore the effect of these treatments on bone healing was studied to clarify the question whether the therapy could be continued after the fracture occurred. This situation is often observed in clinical practice in cases of patients under anti-osteoporotic treatment who experience osteoporotic fracture. The effect of 8-PN and vibration on the spine and femur structure as a part of this study has been published recently (Hoffmann et al., 2016b).

2. Materials and methods

2.1. Experimental design

The animal study protocol was approved by the local regional government in accordance with German animal protection laws prior to performing the study.

Ninety Sprague-Dawley female rats (Harlan-Winkelmann, Borchen, Germany), 12 weeks of age, were divided into seven groups (Fig. 1). After a 5-day acclimatization period, the rats of 6 groups ($n = 78$) were bilaterally Ovx under ketamine (Medistar, Aschenberg, Germany) and xylazine (Ecuphar GmbH, Greifswald, Germany) anesthesia (115 and 8 mg/kg BW, respectively). During the operation, a microchip (UNO PICO ID ISO Transponder, 1.25 × 7 mm, UNO BV, Netherlands) was implanted subcutaneously (s.c.) into each rat for future identification. When the rats were undergoing Ovx, three rats died due to anesthesia-related complications. Rats in the Non-Ovx group were anesthetized, and only electronic chips were implanted (Group 1, $n = 12$).

Five weeks after Ovx, the Ovx rats developed osteoporosis (Kalu, 1991) that was also confirmed by peripheral quantitative computed tomography of lumbar spine in this study (Fig. 6D,G). Thereafter, the treatments were started according to the experimental design (Fig. 1). The groups were designed as follows: Group 1: untreated Non-Ovx rats, Group 2: untreated Ovx rats, Group 3: Ovx rats undergoing vibration treatment (Ovx + Vib), Group 4: Ovx rats treated with alendronate (Ovx + ALN), Group 5: Ovx rats treated with ALN and vibration (Ovx + ALN + Vib), Group 6: Ovx rats treated with 8-PN (Ovx + 8-PN), and Group 7: Ovx rats treated with 8-PN and vibration (Ovx + 8-PN + Vib). All rats received standard soy-free diet (Ssniff special diet GmbH, Soest, Germany) and tap water without restrictions throughout the experiment. Rats were housed three to four in standard rat cages. They were allowed to move freely within the cages at all times. Food intake and body weight of the rats were recorded every week. The rest of the food in the cage was weighed and average daily food intake was calculated dividing the weight of the remaining food by 7 days and the number of rats in the cage (Komrakova et al., 2018).

ALN (Alendronsaure-Ratiopharm®; Ratiopharm GmbH, Ulm, Germany) was mixed with food at a concentration of 10 mg/kg soy-free diet and was given to the rats in Groups 4 and 5. The average daily dosage was 0.58 mg/kg body weight (BW), which was calculated on the basis of average daily food intake in the cage and the individual weight of the rat on the respective day (Fig. 2C). This dosage was reported to have favorable effect on bone tissue and its healing (Kolios et al., 2010).

Rats in Groups 6 and 7 were treated with 8-PN applied daily s.c. by injections at a dosage of 1.77 mg/kg BW (Mukai et al., 2012; Hümpel et al., 2005a 2005b). The dosages in the previous studies ranged from 1.77 mg/kg to 68 mg/kg (Sehmisch et al., 2008; Mukai et al., 2012; Hümpel et al., 2005b; Miyamoto et al., 1998; Štulíková et al., 2018). The higher dosages, however showed strong estrogenic effect in uterus and therefore they are not advisable because of the risk for endometrial cancer is increased via an ER-α receptor-driven mechanism (Hoffmann et al., 2016b; Zhou and Slingerland, 2014). Therefore, we chose the lowest cancer-safe dosage as well as application route (s.c.) based on the previously published data (Hümpel et al., 2005b). 8-PN (5,7-dihydroxy-2-(4-hydroxy-phenyl)-8-(3-methyl-but-2-enyl)-chroman-4-one) was obtained from the Orgentis Chemicals GmbH (Gatersleben, Germany) as a powder (99% purity). 8-PN was dissolved in 100% ethanol (0.3278 g 8-PN in 2 mL of ethanol), mixed with 160 mL 30% hydroxypropyl-beta-cyclodextrin and stored at −20 °C until usage. For each injection, thawed 0.3 mL solution containing 0.6 mg 8-PN was applied to the rat.

Vibration treatments were applied to the Ovx rats in Groups 3, 5, and 7. The regime was as follows: 0.5 mm amplitude, 35 Hz frequency, 1 *g* acceleration (measured at the bottom of the cage with the aid of monitoring system: SWM 3000, REO Elektronic, Berlin, Germany), 15 min duration, 2 times per day, 5 times per week. Transmitted vibration parameters measured at the back of the rat were: 0.08 mm, 35 Hz, 0.17 *g*. This regime has been reported to have a favorable effect on bone healing (Komrakova et al., 2013), whereas the vibrations of higher frequencies could have an adverse effect on bone healing (Komrakova et al., 2013). Rats (7 or 8 at a time) were vibrated with the aid of the vibration device (Vibta Drehstrom-Vibrationsmotor Typ HVL/HVE, Offenbach, Germany), as described earlier (Komrakova et al., 2013; Komrakova et al., 2017).

Four weeks after these treatments (ALN, 8-PN, and Vib), all rats underwent bilateral osteotomy of the tibiae to mimic the clinical situation, when fracture occurs in osteoporotic patients treated with anti-

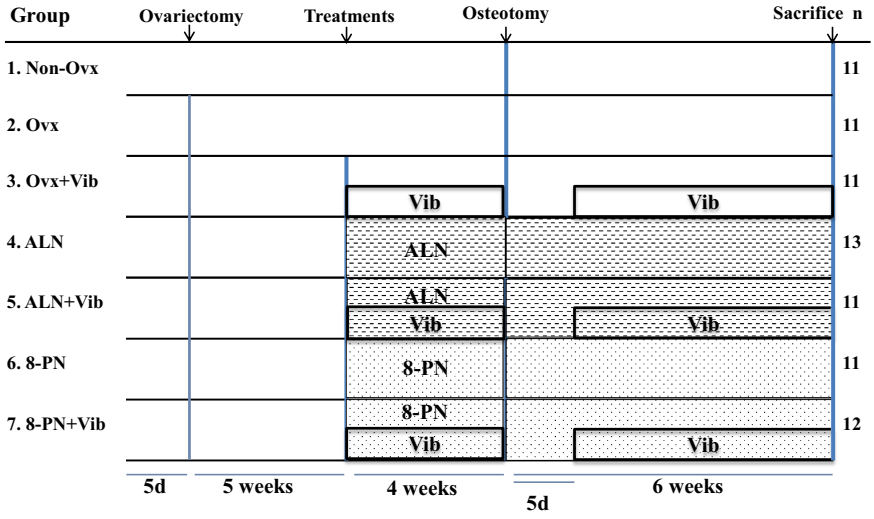

Fig. 1. Schematic flowchart of the experiment. Twelve-week-old female rats were either ovariectomized (Ovx) or left intact (Non-Ovx). Five weeks after the rats were Ovx, the treatments with alendronate (ALN), 8-prenylnaringenin (8-PN), Vibration (Vib) or combined treatments ALN + Vib or 8-PN + Vib were started. Nine weeks after the rats were Ovx, all the rats underwent bilateral osteotomy of the tibia. After osteotomy, Vib treatments were interrupted for 5 days. Samples were analyzed 6 weeks after the osteotomy.

osteoporosis drugs. Tibia osteotomy was performed transversally at the metaphysis as described previously (Komrakova et al., 2018; Stuermer et al., 2010). Briefly, T-shaped titanium plate (57-05140, Stryker Trauma, Selzach, Switzerland) was fixed to the ventro-medial aspect of the tibia with the aid of 4 screws (Stryker Trauma). Thereafter the screws and plate were removed and tibia was osteotomized 7 mm distal to the knee surface using a pulsed ultrasound saw (Piezosurgery®, Mectron Medical Technology, Carasco, Italy). The osteotomy gap of 1 mm was created. Finally, the osteotomized bone ends were fixed with the plate and screws. This method allowed exact reposition of the osteotomized bone. The anesthesia during osteotomy was similar to that used for ovariectomy. Seven rats from different groups died due to anesthesia or surgery-related complications. The final number of enrolled animals is presented in Fig. 1. Treatments with alendronate and 8-PN were continued without interruption, whereas vibration was interrupted for five days after the osteotomy. The welfare of the rats and loading of hind limbs were assessed 3 days before osteotomy operation and daily during 11 days after osteotomy and then twice per week until the end of the experiment as described previously (Komrakova et al., 2018). The differences between the groups were not revealed (data not shown).

For bone-healing analysis, four fluorescent dyes were applied s.c. to the rats (Komrakova et al., 2016). Xylenol orange tetrasodium salt (XO, AppliChem GmbH, Darmstadt, Germany, 90 mg/kg BW) was applied on day 12. Calcein green (CG, Waldeck GmbH & Co KG, Muenster, Germany, 10 mg/kg BW) was applied on day 22. Alizarin-3-methylamine-N·N-diacetic acid dehydrate (AC, Merck, Darmstadt, Germany, 30 mg/kg BW) was applied on day 32, and tetracycline-hydrochloride (TC, Carl Roth GmbH + Co. KG, Karlsruhe, Germany, 25 mg/kg BW) was applied on day 42 after the osteotomy.

2.2. Sample collection

Six weeks after the osteotomy (Fig. 1), the rats were decapitated under CO_2 anesthesia. The uterus was extracted and weighed. Blood serum was collected and stored at −20 °C until analyses of alkaline phosphatase (Alp) using the para-nitrophenyl phosphate method and creatine kinase (Ck) using the *N*-acetyl-L-cysteine method according to the manufacturer's instructions (Architect/Aeroset, Abbott). Serum analyses were conducted at the Department of Clinical Chemistry, University Medical Center, Goettingen, using an automated chemistry analyzer (Architect c16000 analyzer, Abbott, Wiesbaden, Germany).

The musculus gastrocnemius (MG) and musculus soleus (MS) were extracted, weighed and cut in the middle across the muscle. One-half of these muscles and the block (1 cm^3) of musculus longissimus (ML) were covered with talcum powder (AppliChem, Darmstadt, Germany) for histological analyses. Thereafter, the muscles were frozen directly in liquid nitrogen. For the analysis of enzymes, the muscles of the contralateral side were frozen in N_2 without talcum powder. Further storage temperature was −80 °C.

Both tibiae were dissected free of the soft tissues. The osteosynthesis material was removed. Metaphyseal clips of either the left or right tibia, which were chosen randomly, were stored at −80 °C for analysis of gene expression. The contralateral tibia was stored at −20 °C until micro-computed tomographic (micro-CT), biomechanical, and histological analyses.

2.3. Muscle analyses

Muscle samples were cut into serial cross sections of 12-μm thickness using a cryostat (Frigocut 2800E, Leica Biosystems GmbH, Nussloch, Germany) and stored at −20 °C. Air-dried muscle sections were stained for analysis of the capillaries and muscle fibers as described previously (Komrakova et al., 2009).

Muscle capillaries were analyzed using sections fixed in 100% ethanol/chloroform/glacial acid (16:3:1), incubated in 0.3% a-amylase (from porcine pancreas), stained in Schiff's reagent solution (Roth, Karlsruhe, Germany), and treated with 10% potassium sulfite solution (Andersen, 1975). The capillaries and fibers found in two randomly selected fields (0.5 mm^2 each) within a cross section were counted (Suppl. Fig. 1D–G). The ratio of capillaries to muscle fibers was calculated using Excel (MS Office 2010).

For the analysis of muscle fibers, sections were fixed in a 1% paraformaldehyde solution (pH 6.6) containing 1% $CaCl_2$ and 6% sucrose and further stained by incubation in a reduced nicotinamide adenine dinucleotide diaphorase solution (pH 7.4). Then samples were subjected to acidic incubation (pH 4.2) and incubation in adenosine-5′-triphosphate solution (pH 9.4) (Horak, 1983). The muscle fibers were classified as fast-twitch glycolytic (FG), fast-twitch oxidative (FO), and slow-twitch O (SO) types according to Peter et al. (Peter et al., 1972). Cross-sectional areas (CSAs) of at least 90 fibers of each type were determined within three fields of the cross section (1 mm^2 each) (Suppl. Fig. 1A–C). In the MS, only SO fibers were measured given that MS primarily includes these fibers (Hoppeler, 1986).

For the analyses of muscle enzymes, muscle samples were homogenized in ice-cold Chappel-Perry medium (0.1 M KCl, 0.05 M Tris, 0.01 M $MgCl_2$·6 H_2O, 1 mM EGTA, pH 7.5) using a Potter-S-homogenizer (B. Braun Biotech International, Melsungen, Germany). Enzyme activities were assayed using a photometer (LP6; Hach Lange, Duesseldorf, Germany) as described previously (Komrakova et al.,

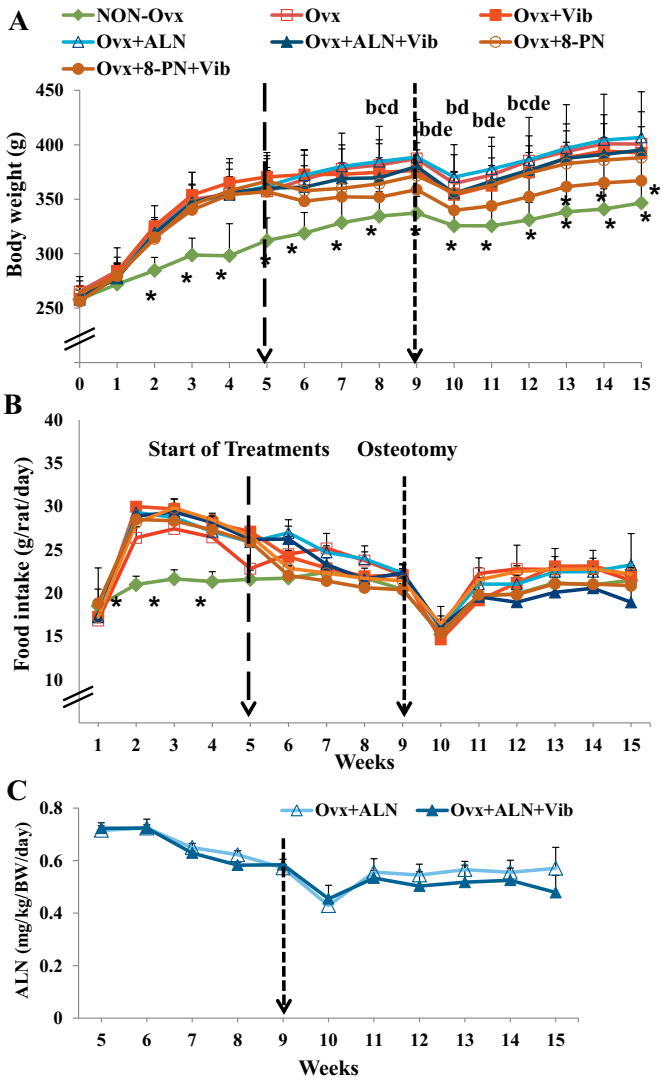

Fig. 2. (A) Body weight of the rats (g) either ovariectomized (Ovx) or left intact (Non-Ovx) at week 0 and treated with ALN, 8-PN, and/or vibration (Vib) during 10 weeks. Mean ± standard deviation (SD) values of at least eleven replications. (B) Food intake of the experimental animals (g/rat/day). (C) ALN doses in ALN treated groups (mg/kg BW/day). Mean ± SD values of three replications. Statistical analysis was done between the treatment groups at the respective week. Asterisk: means of Non-Ovx rats differ from those of the other groups at the respective week. (b–e) Ovx + 8-PN + Vib differs vs. Ovx (b), Ovx + Vib (c), Ovx + ALN (d), Ovx + ALN + Vib (e) ($p < 0.05$, Scheffé-test).

2016). Assays were performed in triplicate. Lactate dehydrogenase (LDH) was measured as described previously (Komrakova et al., 2011a). Citrate synthase (CS) activity was assayed according to Faloona and Srere (1969). Complex I activity was assayed according to Hatefi and Stiggall (1978). The enzyme activity was calculated relative to the protein content. Protein content was determined using aBCATM Protein Assay Kit (Pierce, Rockford, IL, USA), a multilabel reader (Perkin Elmer Precisely Victor X4) and software version 4.0 (Perkin Elmer Life and Analytical Science, Turku, Finland).

2.4. Bone healing analyses

Nondestructive biomechanical analysis was performed using a testing device (Zwick/Roell, type 145660 Z020/TND, Ulm, Germany), as described previously (Komrakova et al., 2015). Briefly, the tibia was loaded at the osteotomy line at the tibial tuberosity. The bending test was stopped before the plastic deformation ended with the bone fracture. Data were recorded with the aid of "testXpert" software (Zwick/Roell). Stiffness (N/mm), which is a slope of the linear rise of the curve during elastic deformation, and yield load, which is end point of elastic deformation (N) defined as a decrease of the curve by more than two standard deviations, were calculated.

Further, the metaphyseal part of the tibia was scanned using an eXplore Locus SP-Scanner (GE Healthcare, London, Ontario, Canada). The scan protocol was as follows: 72 kVp, 90 µA, 1600 ms exposure time, 360° rotation, 0.029 mm voxel size, and 900 projections. Three-dimensional (3D) reconstruction was performed with the aid of the MicroView-Program (v2.1.2, GE Healthcare). The measurement area extended 2.5 mm proximally and distally from the osteotomy line (Suppl. Fig. 2C). The data were converted into bone mineral density (BMD, mg/cm^3) using a linear regression equation formulated by measuring 5 hydroxyapatite standards of several mineral densities. BMD and bone volume fraction (BV/TV) were quantified (Bouxsein et al., 2010).

For histological analyses, the entire tibia was embedded in methyl methacrylate (Merck, Darmstadt, Germany) and cut longitudinally at a thickness of 150 µm using diamond saw microtome (Leica SP 1600, Leica Biosystems GmbH, Nussloch, Germany) (Komrakova et al., 2011b). Three central representative sections were microradiographed with the aid of faxitron Cabinet X-ray system (Hewlett-Packard, Buffalo Grove, IL, USA) using Kodak 100 NIF Industrex Film (SR45, Kodak) and mounted on glass slides with a medium (Eukitt, O Kindler GmbH, Freiburg, Germany). The sections and the corresponding microradiographs were digitalized with the aid of Leica MZ75 microscope and Leica DC 200 digital camera (Leica Microsystems CMS GmbH, Wetzlar, Germany) (Suppl. Fig. 3). The measurements were performed using the QWin image analysis program (Leica). The measurement area extended 2.5 mm proximally and distally from the osteotomy line (Suppl. Fig. 2A,B). The osteotomy gap was divided into the following three regions of interest: 1) craniomedial (cran), plate side 2) caudal (caud), opposite side, and 3) endosteal (e).

The callus area (µm^2) was measured according to fluorescence labeling (Suppl. Fig. 2A). The XO-labeled area was relatively small; therefore, it was measured along with the CG-labeled area. Time of the earliest callus bridging of osteotomy was determined by analyzing the fluorescence labeled sections (at least 10) according to the regions of interest (Komrakova et al., 2016).

Using microradiographs, the cortical width (Ct.Wi) and density (Ct.Dn) distal to the osteotomy line, callus width (Cl.Wi) and density (Cl.Dn) were measured according to the regions of interest (Komrakova et al., 2016) (Suppl. Fig. 2B). Nomenclature used for the histomorphometry was according to Dempster et al. (2012).

Gene expression analysis was performed using quantitative real-time polymerase chain reaction based on SYBR Green detection using iCycler (CFX96, Bio-Rad Laboratories, Munich, Germany). The following genes were analyzed: alkaline phosphatase (Alp), osteocalcin (Oc), tartrate-resistant acid phosphatase (Trap), receptor activator of nuclearfactor k-B ligand (Rankl), and osteoprotegerin (Opg). Ready-to-use primer pairs were obtained from Qiagen (QuantiTect® Primer Assays, Hilden, Germany). Samples were initially homogenized using a microdismembrator S (Sartorius, Goettingen, Germany). Thereafter, cellular ribonucleic acid (RNA) was extracted using the RNeasyTM MiniKit (Qiagen, Hilden, Germany), and then reverse transcribed using SuperscriptTM RNase H-reverse transcriptase (Promega, Mannheim, Germany). The relative gene expression was calculated using the $2^{-\Delta\Delta Ct}$ method (Livak and Schmittgen, 2001). The reference gene was beta-2 microglobulin, and the control group was Non-Ovx.

2.5. pQCT analysis of abdominal CSA and spine

The changes in the abdominal CSA and bone following ovariectomy and treatments were controlled with the aid of peripheral quantitative computed tomography (pQCT), performed in vivo in isoflurane-

anesthetized rats ($n = 5$ per group) using the pQCT device (XCT Research SA, Stratec Medizintechnik GmbH, Pforzheim, Germany). The abdomen of the rat including lumbar spine (lumbar vertebral body L4) was scanned at the beginning of the experiment (prior to Ovx), week 5 after the rats were Ovx (prior to the treatments), week 9 after the rats were Ovx (prior to osteotomy), and at the end of the experiment (15 weeks after Ovx). The scan protocol was as follows: 90 mm measurement diameter, 0.2 mm voxel size, 90 s scan time, 0.3 mA anode current, 50 kV high voltage, 180 projections, and 1° angle between detectors (Komrakova et al., 2016). The bone mineral density (mg/cm^3), stress-strain-index (SSI), and abdominal CSA (mm^2) were assessed with the aid of the XCT-6.20C software (Stratec Medizintechnik GmbH).

2.6. Statistical analyses

Gaussian distribution was tested for each parameter by applying Kolmogorov–Smirnov test, P'Agostino and Person omnibus test, and Shapiro-Wilk test using GraphPad Prism (Version 5.04, GraphPad Software, Inc. San Diego, CA, USA). The data were considered normally distributed if they passed at least one of the normality tests.

One-way ANOVA and the Scheffé-test (SAS program 9.1, SAS Institute, Cary, NC, USA) were used ($p < 0.05$) for normally distributed variables. For not normally distributed variables non-parametric Kruskal-Wallis test and Dunn multiple comparison test ($p < 0.05$) (GraphPad Prism) were applied. Data are shown as means and standard deviations.

3. Results

3.1. Food intake, body weight, and uterus weight

The body weight (BW) of the rats did not differ significantly at the beginning of the experiment (Fig. 2A). Two weeks after the rats were Ovx, BW of all the Ovx rats increased significantly and remained elevated until the end of the experiment. One exception was the BW of rats in the Ovx + 8-PN + Vib group. These rats exhibited a decrease in BW after the 3-week treatment, and the BW was further reduced during the additional treatments weeks. Directly after osteotomy, the BW decreased in all groups; however, weights returned to levels noted prior to osteotomy within the later 3 weeks (Fig. 2A).

The food intake of the Ovx rats increased during the first 2 weeks after they were Ovx (Fig. 2B). Thereafter, it decreased steadily to reach that of Non-Ovx rats. At the beginning of the treatments (5 weeks after the rats were Ovx), the food intake did not differ between the groups. Osteotomy caused a drop in the food intake of all rats. After 2 weeks, the intake increased to the level recorded prior to the operation (Fig. 2B).

The average daily dosage corresponded to the average food intake of the rats throughout the experiment (Fig. 2C). The differences between Ovx + ALN and Ovx + ALN + Vib groups were not significant and the ALN dose averaged 0.58 mg/kg BW.

The uterus weights of the Non-Ovx rats were significantly higher (652 ± 158 mg) than that of all the Ovx groups (Ovx: 108 ± 19 mg, Ovx + Vib: 103 ± 24 mg, Ovx + ALN: 101 ± 35, Ovx + ALN + Vib: 109 ± 32 mg, Ovx + 8-PN: 156 ± 25 mg, Ovx + 8-PN + Vib: 172 ± 31 mg). The differences between the all Ovx groups were not significant (published partly in Hoffmann et al., 2016b).

3.2. Muscle analyses

The capillary ratio of ML was higher in the Ovx + Vib than in the Non-Ovx and Ovx rats (Table 1). Similarly, capillary density was also enhanced in Ovx + ALN group, whereas ALN + Vib treatment did not change it. 8-PN alone did not affect capillarization, whereas 8-PN + Vib treatment decreased capillary density. In MS, the ratio of the capillaries reached significantly higher levels in the Ovx + ALN and Ovx + ALN + Vib and in the Ovx + 8-PN and Ovx + 8-PN + Vib groups compared with the Non-Ovx, Ovx and Ovx + Vib groups. In MG, the differences were not detectable.

The changes in the cross sectional area (CSA) of muscle fibers are presented in Fig. 3(A–G). In MG, the CSA of fast-twitch oxidative (FO) and fast-twitch glycolytic (FG) muscle fibers was reduced in the Ovx + 8-PN and Ovx + 8-PN + Vib rats compared with other ovariectomized groups (Fig. 3B, C). In ML, Ovx + Vib rats exhibited the largest CSA of slow-twitch (SO) fibers (Fig. 3D). The CSA of FG was increased in the Ovx + Vib and Ovx + ALN groups compared with Non-Ovx rats. In the Ovx + 8-PN group, the CSA of FG was reduced compared with the Ovx + Vib group (Fig. 3F). In MS, the CSA of SO did not differ between the groups (Fig. 3G).

Enzyme analysis revealed enhanced activity of lactate dehydrogenase (LDH) in the MS of the Ovx + ALN and Ovx + ALN + Vib groups (Table 1). Citrate synthase (CS) and Complex I activities did not differ between the treatment groups in any of the three muscles studied (Table 1).

The weight of MG was lower in the Non-Ovx and Ovx + 8-PN + Vib groups compared with the other groups (Fig. 3G). Similarly, the weight of MS was reduced in these groups; however, it did not reach a significant level (Fig. 3H).

3.3. Bone healing analyses

Biomechanical parameters of the tibia were not significantly different between the groups, probably due to high standard deviations (Table 2).

Micro-CT analysis of tibia at the osteotomy site revealed lower BMD and BV/TV in all the Ovx groups compared to those in the Non-Ovx group (Fig. 4A,B). The exception was the Ovx + ALN + Vib group. In this, BV/TV increased to the level observed in the Non-Ovx rats (Fig. 4A).

An analysis of microradiographs is shown in Fig. 4(C–I). Ovx negatively affected most of the bone parameters. Vib alone increased the callus width and decreased its density (Fig. 4F,I). ALN had no effect on the callus width and density (Fig. 4E–I), while caudal cortical width was decreased (Fig. 4C). Combined treatment ALN + Vib caused increased callus width and density with decreased cortical width (Fig. 4C–E,H,G). 8-PN treatment enlarged the callus width, whereas cortical width and callus density were diminished (Fig. 4C–E,G,I). 8-PN + Vib decreased the cortical width compared to 8-PN (Fig. 4D). Callus density was lower in Ovx + 8-PN + Vib compared with the Non-Ovx and Ovx groups (Fig. 4I). Cortical density did not differ significantly among the treatment groups (overall mean craniomedial: 98.2% + 0.5% and caudal: 98.7% + 0.4%).

Analysis of the fluorochrome-labeled sections showed that in Non-Ovx rats, a significantly larger callus area was built endosteally during the first 22 days of healing compared with that in the other groups (Fig. 5C, CG staining). Vib treatment alone enlarged total caudal area in Ovx rats (Fig. 5D). ALN increased craniomedial callus formation during the last 20 days of bone healing (Fig. 5A, AC and TC staining). Combined treatment ALN + Vib increased AC callus areas endosteal compared with that in Non-Ovx group (Fig. 5C) and the total callus area compared with Non-Ovx and Ovx groups (Fig. 5D). Similarly, 8-PN alone treatment caused a significant enlargement of total callus area (Fig. 5D). In both groups (Ovx + ALN + Vib and Ovx + 8-PN), this effect was observed mostly on the formation of the caudal callus during the first 32 days following osteotomy (CG and AC staining, Fig. 5B). Combined 8-PN and Vib treatment reduced callus formation (Fig. 5B–D).

Bridging of osteotomy was observed in all rats. It occurred earlier in the Non-Ovx rats compared with all Ovx rats irrespective of the treatments (Table 2).

Alp gene expression was enhanced in the Ovx + ALN and Ovx + ALN + Vib groups compared with the Non-Ovx and Ovx + Vib

Table 1
Muscle analyses. Activity of the muscle enzymes: lactate dehydrogenase (LDH), citrate synthase (CS), and Complex I, and number of capillaries per muscle fiber in muscularis longissimus (ML), muscularis soleus (MS), and muscularis gastrocnemius (MG) of Non-Ovx or Ovx rats treated with ALN, 8-PN, and/or vibration (Vib) during 10 weeks.

Parameters	Non-Ovx		Ovx		Ovx + Vib		Ovx + ALN		Ovx + ALN + Vib		Ovx + 8-PN		Ovx + 8-PN + Vib	
	Mean	SD	Mean	SD	Mean	SD	Mean	SD	Mean	SD	Mean	SD	Mean	SD
ML														
LDH	3.40	0.56	3.72	0.94	3.59	1.23	4.24	0.93	4.36	1.22	3.61	0.96	3.74	0.56
CS	58.3	10.5	56.9	15.3	57.2	22.6	65.1	20.9	64.4	14.5	54.4	13.6	66.1	17.9
Complex I	10.5	2.1	11.4	3.0	9.8	4.5	10.0	4.7	8.7	4.3	7.6	2.6	11.2	3.8
Capillaries/fiber	1.13	0.22	1.16	0.24	1.30[ab]	0.23	1.34[ab]	0.31	1.26	0.18	1.23	0.24	1.09[cdef]	0.16
MS														
LDH	0.87	0.22	1.04	0.20	0.97	0.14	1.28[ac]	0.32	1.18[a]	0.24	0.99[d]	0.25	0.96[d]	0.22
CS	85.1	20.4	86.8	16.6	94.3	17.7	99.4	22.3	87.9	17.5	95.7	12.8	96.9	7.5
Complex I	21.2	5.7	18.3	11.4	18.6	7.4	19.1	5.6	17.2	7.7	13.2	4.5	16.5	3.8
Capillaries/fiber	1.19	0.22	1.27	0.29	1.34	0.15	1.68[abc]	0.29	1.78[abc]	0.3	1.80[abc]	0.20	1.80[abc]	0.40
MG														
LDH	3.52	1.07	4.12	0.70	3.34	0.59	4.25	0.69	3.38	0.69	3.67	0.42	3.56	0.58
CS	66.8	20.7	62.8	19.5	66.1	31.6	67.1	26.5	68.6	15.8	79.5	28.6	71.0	17.2
Complex I	13.2	4.9	11.2	4.5	8.6	5.6	11.4	6.1	11.8	8.2	7.3	3.7	10.4	3.7
Capillaries/fiber	1.32	0.26	1.35	0.38	1.35	0.32	1.43	0.28	1.39	0.38	1.42	0.39	1.34	0.35

At least ten replications per group were done. SD: standard deviation.
Mean with superscripts differ significantly: [a]vs. Non-Ovx, [b]vs. Ovx, [c]vs. Ovx + Vib, [d]vs. Ovx + ALN, [e]vs. Ovx + ALN + Vib, [f]vs. Ovx + 8-PN ($p < 0.05$). Dunn-test: Complex I in MS, LDH in MG. Scheffé-test: all other parameters.

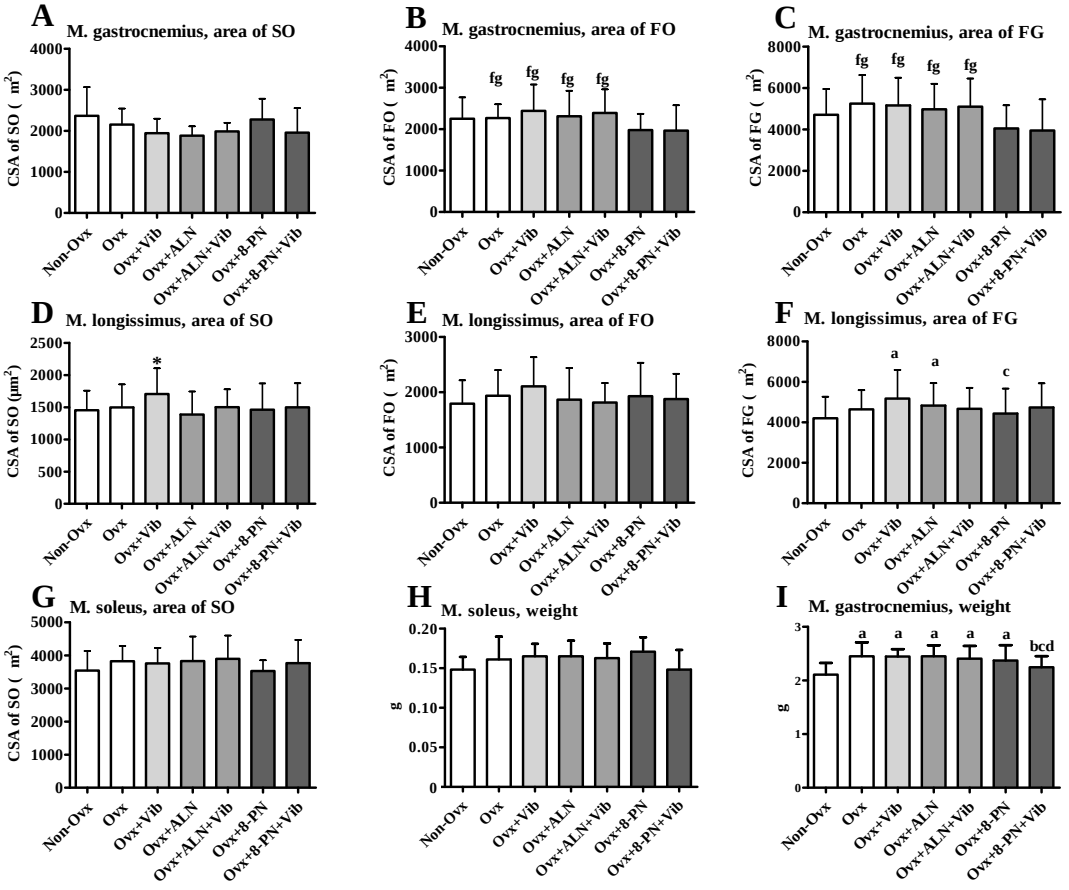

Fig. 3. Cross-sectional area of slow-twitch oxidative (SO) (A,D,G), fast-twitch oxidative (FO) (B,E), and fast-twitch glycolytic (FG) (C,F) muscle fibers in musculus soleus (MS), musculus gastrocnemius (MG), and musculus longissimus (ML), as well as the weight of MS (H) and MG (I). Mean ± standard deviation (SD) values of at least eleven replications. (a) Means differ vs. Non-Ovx, (b) vs. Ovx, (c) vs. Ovx + Vib, (d) vs. Ovx + ALN, (f) vs. Ovx + 8-PN, (g) vs. Ov + -PN + Vib ($p < 0.05$). Dunn-test: A,C,E. Scheffé-test: B,D,F–I.

Table 2
Tibia analyses. Biomechanical analysis, day of osteotomy bridging, serum analysis and gene expression analysis in Non-Ovx rats or Ovx rats treated with ALN, 8-PN, and/or vibration (Vib) during 10 weeks.

Parameters	Non-Ovx		Ovx		Ovx + Vib		Ovx + ALN		Ovx + ALN + Vib		Ovx + 8-PN		Ovx + 8-PN + Vib	
	Mean	SD	Mean	SD	Mean	SD	Mean	SD	Mean	SD	Mean	SD	Mean	SD
Biomechanics														
Stiffness (N/mm)	90	50	55	31	49	36	48	40	51	19	51	19	47	27
Yield load (N)	59	35	53	31	38	32	36	26	32	10	31	12	35	19
Day of bridging	21	7	26	7	25	9	29	10	25	5	27	7	27	8
Serum analyses														
Total Alp (U/L) (Hoffmann et al. 2016b)	91	15	113	18	150[ab]	34	112[ce]	12	150[ab]	19	137[a]	28	136[a]	8
Ck (U/L)	7903	1679	8220	2127	7506	1339	7466	1715	8078[a]	1371	6517	1655	5269[b]	2483
Gene expression ($2^{-\Delta\Delta CT}$) at the osteotomy site														
Alp	1.03	0.22	1.39	0.56	0.99	0.27	1.93[ac]	0.48	1.85[ac]	0.76	1.38[abd]	0.60	1.55	1.10
Oc	0.88	0.64	0.84	0.30	0.41	0.10	0.60	0.36	0.74	0.31	1.18	0.38	0.89	0.55
Trap	1.08	0.52	1.40	0.63	1.02	0.34	1.15	0.68	1.96	1.24	1.31	0.77	0.97[bde]	0.49
Opg	1.07	0.41	0.92	0.27	1.16	0.40	0.72	0.41	1.59[abd]	0.78	0.69[e]	0.37	1.01[e]	0.34
Rankl	1.07	0.41	2.80[a]	1.01	2.11[a]	1.17	2.20[a]	0.69	2.92[a]	1.32	1.22[bde]	0.43	1.64[be]	0.52
Opg/Rankl	1.17*	0.60	0.36	0.17	0.61	0.22	0.35	0.10	0.57	0.23	0.56	0.21	0.64	0.18

At least ten replications per group were done. SD: standard deviation.
Mean with superscripts differ significantly: *vs. others, [a]vs. Non-Ovx, [b]vs. Ovx, [c]vs. Ovx + Vib, [d]vs. Ovx + ALN, [e]vs. Ovx + ALN + Vib ($p < 0.05$). Dunn-test: Stiffness, Ck. Scheffé-test: all other parameters.

groups (Table 2). Opg mRNA expression was at the highest level in the Ovx + ALN + Vib group. Rankl gene expression was higher in the Ovx, Ovx + Vib, Ovx + ALN, and Ovx + ALN + Vib groups compared with the Non-Ovx group. In contrast, Ovx + 8-PN and Ovx + 8-PN + Vib treatments lowered it to the level observed in the Non-Ovx rats. The ratio of Opg/Rankl was higher in the Non-Ovx group compared with other groups. OC and Trap expression did not differ among the groups (Table 2).

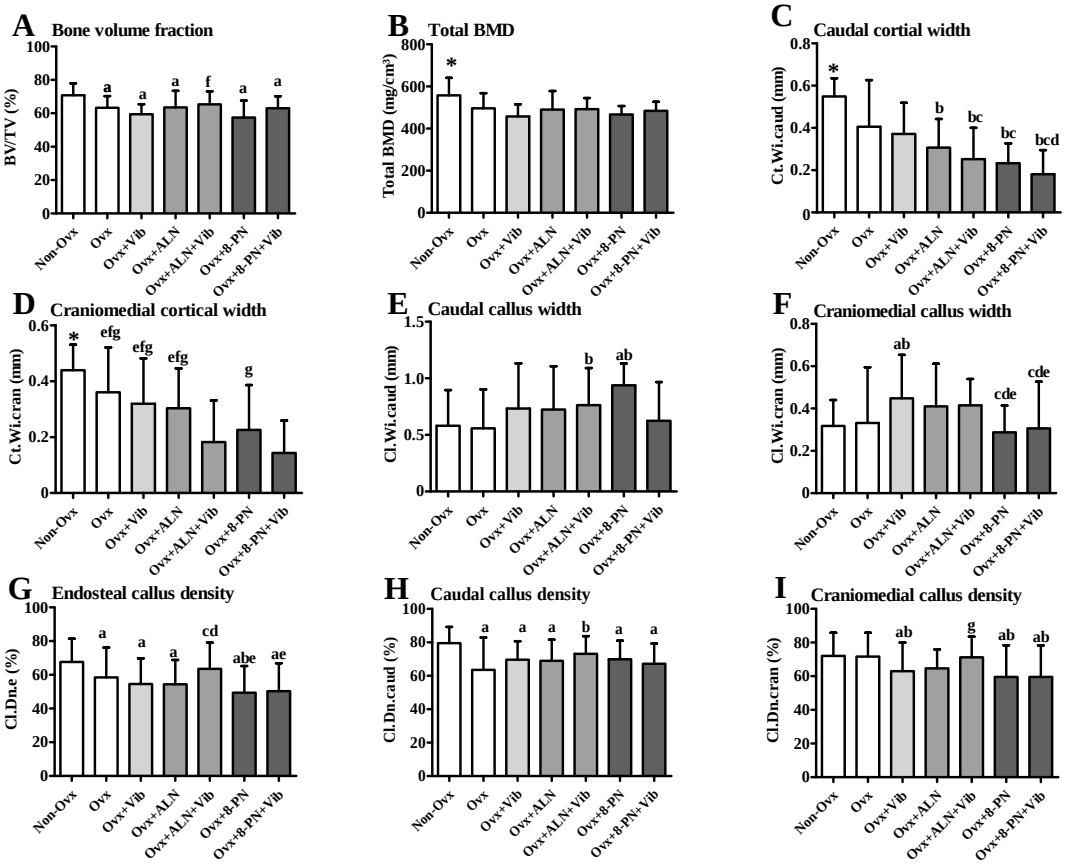

Fig. 4. Analyses of micro-CT (A,B) and the microradiographs (C–I) of tibiae made at the osteotomy site divided into craniomedial (cran), caudal (caud) and endosteal (e) regions in Non-Ovx and Ovx rats treated with ALN, 8-PN and/or Vib during 10 weeks. Cl: Osseous callus tissue, Ct: Cortical bone, Wi: Width, Dn: Density, BV/TV: Bone volume fraction, Total BMD: Total bone mineral density. Means ± SD of at least eleven replications. (a) means differ vs. Non-Ovx, (b) vs. Ovx, (c) vs. Ovx + Vib, (d) vs. Ovx + ALN, (e) vs. Ovx + ALN + Vib, (f) vs. Ovx + 8-PN, (g) vs. Ovx + 8-PN + Vib ($p < 0.05$). Dunn-test: E–G. Scheffé-test: A–D,H,I.

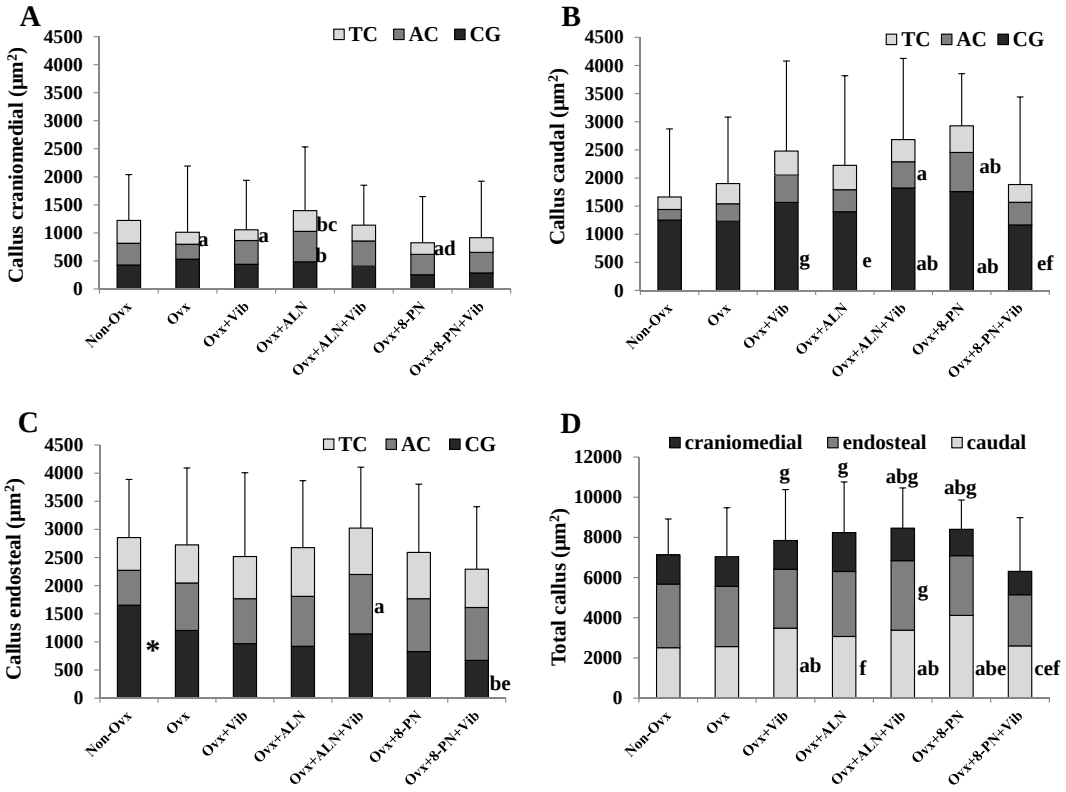

Fig. 5. Callus area (µm^2) measured in fluorescence-labeled sections of the tibia divided into craniomedial (A), caudal (B), and endosteal (C) regions in Non-Ovx and Ovx rats treated with ALN, 8-PN and/or Vib. (D) Total callus area (µm^2). CG: calcein green stained callus area built within 0–22 days, AC: alizarin complexon stained area built within 23–32 days, TC: tetracycline stained area formed within 33–41 days after osteotomy. Means ± SD of at least eleven replications. Asterisk: means differs from all other groups, (a) vs. Non-Ovx, (b) vs. Ovx, (c) vs. Ovx + Vib, (d) vs. Ovx + ALN, (e) vs. Ovx + ALN + Vib, (f) vs. Ovx + 8-PN, (g) vs. Ovx + 8-PN + Vib ($p < 0.05$). Scheffé-test: CG endosteal, CG caudal, total caudal. Dunn-test: all other parameters.

3.4. pQCT analysis of the abdominal CSA and the spine

Abdominal CSA at the beginning of the study did not differ between the groups and was 1361 ± 101 mm^2 on average ($n = 5$ per group). Five weeks after the rats were Ovx, all the Ovx rats had a larger CSA than the Non-Ovx rats (Fig. 6A). Nine and fifteen weeks after the rats were Ovx, the highest CSA remained only in the Ovx group (Fig. 6B,C). In the Ovx + 8-PN and Ovx + 8-PN + Vib groups, the CSA was similar to that in the Non-Ovx rats. At the end of the experimental period, all the treatments (excluding Ovx) caused a significant reduction in CSA. The lowest CSA was noted in the Ovx + 8-PN + Vib group (Fig. 6C).

Total BMD and SSI of the lumbar vertebral body did not differ between the groups prior to Ovx averaging 506 ± 25 mg/cm^3 and 11 ± 2 mg/cm^3, respectively (n = 5 per group). At the beginning of the treatments (5 weeks after the rats were Ovx), these parameters were significantly lower in all the Ovx groups than in the Non-Ovx group (Fig. 6D,G). Four weeks of treatments did not change these differences (Fig. 6E,H). After ten weeks of treatments, the BMD and SSI of the Non-Ovx rats remained at the highest level (Fig. 6F,I). In the Ovx + Vib and Ovx + 8-PN groups, these parameters were reduced.

3.5. Serum analyses

The serum Ck was significantly lower in the 8-PN + Vib group than that in the Ovx group (Table 2). Between other groups the differences were not significant. Serum Alp increased significantly in Ovx and ALN groups treated with Vib (Table 2). In the non-vibrated Ovx and ALN groups, it was at the level of the Non-Ovx group (Hoffmann et al., 2016b). In both 8-PN treated groups, the serum Alp level was higher than that in Non-Ovx group (Hoffmann et al., 2016b).

4. Discussion

We investigated the changes in the muscle structure and bone healing in ovariectomy-induced osteopenic rats treated with ALN or 8-PN alone or in combination with vibration. Ovariectomy was confirmed by reduced uterus weight, increased body weight (Hoffmann et al., 2016b) and increased abdominal CSA in Ovx rats compared with Non-Ovx rats. Impaired bone parameters of lumbar spine and increased body weight and abdominal CSA were observed 5 weeks after the ovariectomy, i.e., prior to treatment initiation. These changes have been previously reported in mature female rat after ovariectomy (Kalu, 1991; Komrakova et al., 2009; Lei et al., 2009).

Depletion of hormones caused an increase in the muscle weight of the Ovx rats, whereas the treatments did not affect weight in general. The exception was the combined treatment of 8-PN and vibration. In these rats, the weight of MG decreased to a level similar to that in intact Non-Ovx rats. These observations could be explained by the changes in BW. A strong correlation of body weight and muscle weight has been previously reported (Komrakova et al., 2016).

In Ovx rats, bone healing was impaired. We observed decreased BV/TV, BMD, cortical width, callus density, and endosteal callus formation in Ovx rats. These findings are in agreement with previous reports of impaired mineralization and callus structure and diminished biomechanical properties in the Ovx rats (Komrakova et al., 2016; Namkung-Matthai et al., 2001; Yingjie et al., 2007). The bone biomechanical properties of the Ovx rats in the present study were also diminished at the osteotomy site; however, the differences did not reach statistical significance.

The application of vibration alone increased the CSA of the muscle fibers and the capillary density in ML. In other muscles, the effect of the vibration was less pronounced. Our results confirm previous reports

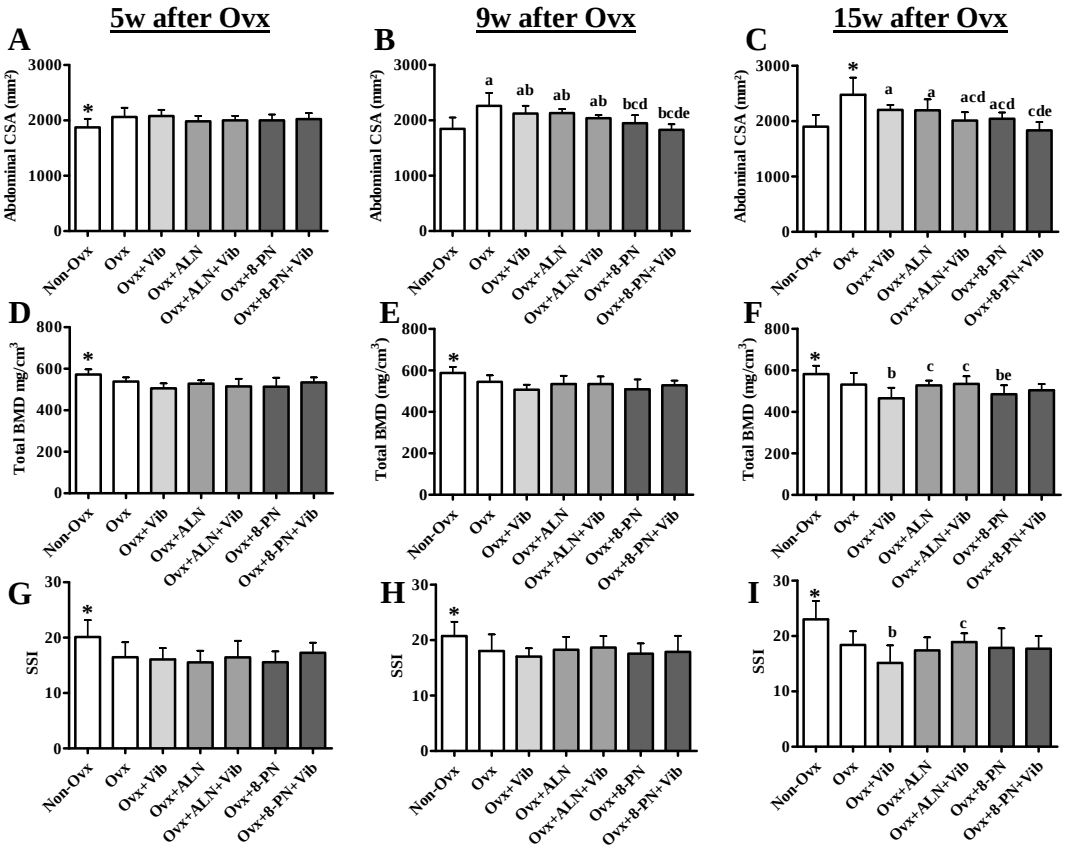

Fig. 6. Results of the peripheral quantitative computed tomography (pQCT) measurements of the vertebrae (D–I) and abdominal CSA (A–C) in vivo at the beginning of the study, at 5 (A,D,G), 9 (B,E,H) and 15 (C,F,I) weeks. At the beginning of the study, CSA: 1361 ± 101 mm^2, total BMD: 506 ± 25 mg/cm^3, SSI: 11 ± 2. Asterisk: means of Non-Ovx rats differed from those of the other groups, (a) vs. Non-Ovx, (b) vs. Ovx, (c) vs. Ovx + Vib, (d) vs. Ovx + ALN, (e) vs. Ovx + ALN + Vib ($p < 0.05$, Scheffé-test).

that have demonstrated a significant increase in the muscle fiber size and blood supply following treatments with vibrations (Komrakova et al., 2013, 2016; Xie et al., 2008) and different responses of various muscles to these treatments (Komrakova et al., 2016). Vibration exerts beneficial effects on the neuromuscular system; this may be attributed to the enhanced electrical activity of the muscles (Karacan et al., 2017). Furthermore, in addition to ER, the receptors of muscle spindle, golgi tendon organs, or somatosensory receptors respond to oscillatory stimuli (Fallon and Macefield, 2007).

In osteotomized tibia, vibration caused an enlargement of the periosteal callus area and width, a decrease in the callus density and an increase in serum Alp activity. These observations indicate that the vibration applied in the present study interferes with early bone healing that is in accordance with some of the studies (Komrakova et al., 2016; Wang et al., 2017). However, other studies showed a positive effect of vibration on bone healing (reviewed in Wang et al. (2017)). In the previous studies, the parameters such as fracture model and fixation type (diaphysis or metaphysis, tibia, femur, fibula or rib, external or internal), age of the animals (4 weeks to 9 months), vibration regimes (frequency, duration) and time point of bone healing studied (9 to 56 days) were various and also different from those applied in our study (Wang et al., 2017). In the present study, the vibration treatment had an impact not only on the osteotomized bone but also diminished bone parameters of the lumbar spine as it was shown by pQCT analysis and previous structural analysis (Hoffmann et al., 2016b).

ALN enhanced the capillary density in ML and MS and the activity of LDH in MS, and reduced abdominal CSA. The effect of ALN on body and muscle weight and muscle fiber CSA was not observed. The combined treatment of ALN and vibration did not change the effect of ALN. The effect of ALN on muscle structure and muscle capillarization has been not reported to date. In contrast to our findings, other in vitro and in vivo studies have suggested that bisphosphonates elicit anti-angiogenic effects through several mechanisms that could explain their antitumoral action (Giraudo et al., 2004; Ferretti et al., 2005; Petcu et al., 2012). Treatments with bisphosphonates induce inhibition of insulin-like growth factor 1 (IGF-1) and reduction in vascular endothelial growth factor (VEGF), basic fibroblast growth factor (FGF-2), matrix metalloproteinase-2 (MMP-2) and matrix metallopeptidase 9 (MMP-9) in breast cancer cells and angiogenic endothelial cells in patients with metastatic breast cancer and in biopsies of bisphosphonate-related osteonecrosis of jaw (Giraudo et al., 2004; Ferretti et al., 2005; Petcu et al., 2012). Another adverse effect of ALN therapy is muscle pain (Tienboon and Jaruwangsanti, 2014). In the present study, LDH enzyme activity was enhanced in MS after both ALN treatments. It was also enhanced in the other two muscles studied; however, this increase was not statistically significant. LDH is involved in anaerobic glycolysis. The elevated activity of LDH has been reported in numerous muscle disorders characterized by myonecrosis (Valberg, 2008). Thus, our findings indicate that anti-osteoporosis therapy with ALN affects muscle capillarization and metabolism. However, the effect remains unclear and warranted further investigations.

In the tibia, ALN treatment enhanced the late callus formation and diminished cortical width at the end of the study. The occurrence of bone bridging in ALN group was observed at the latest date. This finding may indicate delayed bone healing which occurred at the early stages of healing and was compensated by enhanced callus formation at the late stages. Different effects of bisphosphonates on bone healing have been reported. Some researchers found that alendronate strongly

suppressed remodeling of the callus, resulting in a large amount of woven bone in Ovx rats (Cao et al., 2002); however, others suggest that alendronate improves callus properties (Kolios et al., 2010). Currently, bisphosphonates are not prescribed for patients with fractures during bone healing.

ALN applied in combination with vibration significantly increased the callus width and density, enhanced callus formation during the earlier stage of healing, and reduced cortical width. Corresponding to the changes in the bone, serum Alp activity was enhanced and Alp, Opg, and Rankl gene expression was up regulated. This finding may indicate accelerated bone resorption and formation rates in Ovx + ALN + Vib rats. These results confirm a previous report of significant enhancement in the ALN effect by vibration via improvements in the biomechanical and structural properties of the non-osteotomized tibia of the Ovx rats (Chen et al., 2014). In addition, lumbar spine BMD and SSI were unaltered after both the ALN treatments in the present study.

Thus, both ALN treatments affected muscle tissue by enhancing capillarization and LDH activity. ALN applied alone slowed bone healing, whereas the combined therapy of ALN and vibration improved it.

In both the 8-PN groups, a decrease in the CSA of the FO and FG muscle fibers in MG and in the abdominal CSA as well as an increase in the capillary density in MS was observed, irrespective of the vibration treatment. 8-PN is a phytoestrogen (Mukai et al., 2012), and its effect observed on muscle structure and abdominal CSA may be attributable to its estrogenic activity. Estrogen reportedly stimulates angiogenesis in the skeletal muscles (Kyriakides et al., 2001) and has an effect on BW and body composition independently of food intake (Komrakova et al., 2009; Toth et al., 2001). However, the combination of 8-PN and vibration changed the effect of 8-PN on some other muscle parameters. This difference is demonstrated by reduction in BW, muscle weight, abdominal CSA, capillary density in ML, and serum Ck activity to the level observed in the Non-Ovx rats. Both 8-PN and vibration treatments stimulate ERα, which are found in the skeletal muscle (Milligan et al., 2002; Keiler et al., 2013; Wiik, 2008; Wehrle et al., 2015b). It could be assumed that vibration, in combination with 8-PN exerted a synergistic effect by stimulating the ERα in the muscle of the Ovx rats. Furthermore, estrogen influences BW, and vibration exercises suppress fat accumulation in adult rats (Maddalozzo et al., 2008). Reduced Ck levels potentially resulted from the reduced muscle mass (Rosalski, 1998) in the 8-PN + Vib group in the present study. The enhanced serum Ck level is instead indicative of various muscle pathological processes, such as injury, myocardial infarction, and muscular dystrophy. Differences in the responses of capillary density of limb muscle (MG) and back muscle (ML) to the combined treatment of 8-PN and vibration could be due to the differences in the muscle functions, different transmissions of the vertical vibration, and/or to the possible effect of tibia osteotomy on the surrounding muscle tissue.

In tibia, 8-PN increased the callus width. However, the callus density and cortical width were decreased after this treatment. Analysis of the fluorescence-labeled callus revealed a larger callus area at the caudal aspect during early healing (CG and AC staining). 8-PN has been reported to promote osteoblastic bone formation and inhibit osteoclastic bone resorption; its effect is reported to be mediated by ERα in vitro (Luo et al., 2014). In fact, Rankl mRNA expression was reduced in both the 8-PN groups. This feature may decelerate callus remodeling by inhibiting osteoclastogenesis. pQCT analysis of the lumbar spine in the present study and additional data in its detailed analyses (Hoffmann et al., 2016b) revealed unfavorable effects of 8-PN on bone parameters in the Ovx rats applied in this study as osteoporosis therapy. In previous studies that showed favorable effect of 8-PN on bone tissue, it was applied as osteoporosis prophylaxis, i.e., immediately after Ovx (Sehmisch et al., 2008; Hümpel et al., 2005b). This could explain the different effects of 8-PN treatments on bone of Ovx rats.

The combined 8-PN and vibration treatment demonstrated an effect contradictory to that of 8-PN alone in tibia; it decreased the callus width and area. It may be hypothesized that the loading of the callus was different in these two groups given the reduced body and muscle weight of the Ovx + 8-PN + Vib rats compared to the Ovx + 8-PN group rats. Weight bearing and mechanical loading are important for adequate fracture healing and callus formation (Komrakova et al., 2018; Rueff-Barroso et al., 2008). The loss of BW is associated with the loss of visceral fat that influences the levels of circulating estrogen and other sex hormones; it may also reduce bone mass and density (Shapses and Riedt, 2006) and influence bone healing. On the other hand, these rats were exposed to vibration that stimulated callus remodeling so that the formed callus was resorbed at a higher rate.

In summary, in both the 8-PN groups, the CSA of the muscle fibers was reduced, whereas the capillary density was increased. These results underscore the positive effect of 8-PN on the muscle tissue in Ovx rats. In the tibia, callus density, cortical width, and Rankl gene expression were reduced at the osteotomy site irrespective of the changes in callus width and area. This finding indicates an unfavorable effect of 8-PN on bone healing.

5. Conclusion

Vibration, applied as a single therapy, was beneficial for muscle structure; however, it tended to interfere with early bone healing. ALN enhanced capillary density and LDH activity in muscles, thus having an impact on the muscle blood supply and metabolism irrespective of the vibration treatment. Further studies are warranted to investigate how these changes can affect muscle function. In the tibia, ALN slowed bone healing. 8-PN alone exerted favorable effects on muscle structure but proved disadvantageous for bone healing.

Although the vibration regime in the present study was identical for all rats, its effect differed if the vibration was applied as a single therapy or in combination with ALN or 8-PN. ALN + Vib improved bone healing; however, 8-PN + Vib worsened the effect of 8-PN treatment alone on the bone. The drastic loss of body and muscle weight in the Ovx + 8-PN + Vib group likely exerted a negative effect on the musculoskeletal system in the Ovx rats.

Thus, vibration, ALN, 8-PN, or 8-PN + Vib treatments do not seem advisable during the early bone-healing period. Though our data suggest that ALN + Vib treatment may be continued after a fracture, there is a concern about its application since the single treatments showed negative effects on bone healing.

In conclusion, we demonstrated that the muscle tissue responded to the anti-osteoporosis treatments, and the responses differed in some aspects, based on the effects observed in the bone. Therefore, analyses of not only the bone tissue but also the muscle tissue are recommended for the evaluation of anti-osteoporosis drugs. Improvements in the bone and musculature would prevent falls and reduce the fracture risk, thereby improving the quality of life and mobilization of osteoporotic patients. Further studies including continuous monitoring at different time points of bone and muscle structure, function and metabolism may help our understanding of the effect of different treatments on musculoskeletal system.

6. Limitations

In the present study, 8-PN was injected s.c., whereas other treatment groups received no injections. Although the welfare of the rats treated with 8-PN did not differ from other animals in general, it is important to note that excessive handling required for the animals in 8-PN treated groups might have an effect on limb loading and fracture healing progression.

The biomechanical test was performed using frozen-thawed tibiae according to the experimental protocol and related workflow. Though all samples were handled in the same way, the storage of bone could affect the results and may contribute to the high variation in the biomechanical data.

Supplementary data to this article can be found online at https://doi.org/10.1016/j.bonr.2019.100224.

Transparency document

The Transparency document associated with this article can be found, in the online version.

Acknowledgments

This study was supported by the German Research Foundation (DFG, SE 1966/5-1). The authors are grateful to their colleagues R. Castro-Machguth, and A. Witt for their technical support. We also acknowledge support by the Open Access Publication Funds of the Göttingen University.

References

Andersen, P., 1975. Capillary density in skeletal muscle of man. Acta Physiol. Scand. 95, 203–205.

Anderson, G.L., Limacher, M., Assaf, A.R., Bassford, T., Beresford, S.A., Black, H., Bonds, D., Brunner, R., Brzyski, R., Caan, B., Chlebowski, R., Curb, D., Gass, M., Hays, J., Heiss, G., et al., 2004. Effects of conjugated equine estrogen in postmenopausal women with hysterectomy: the Women's Health Initiative randomized controlled trial. Jama 291, 1701–1712.

Bosco, C., Colli, R., Introini, E., Cardinale, M., Tsarpela, O., Madella, A., Tihanyi, J., Viru, A., 1999. Adaptive responses of human skeletal muscle to vibration exposure. Clin. Physiol. 19, 183–187.

Bouxsein, M.L., Boyd, S.K., Christiansen, B.A., Guldberg, R.E., Jepsen, K.J., Müller, R., 2010. Guidelines for assessment of bone microstructure in rodents using micro-computed tomography. JBMR 25, 1468–1486.

Burr, D.B., 1997. Muscle strength, bone mass, and age-related bone loss. JBMR 12, 1547–1551.

Campos, J.F., Mierzwa, A.G.H., Freitas-Jesus, M., Lazaretti-Castro, M., Nonaka, K.O., Reginato, R.D., 2018. Mechanical vibration associated with intermittent PTH improves bone microarchitecture in ovariectomized rats. J. Clin. Densitom. https://doi.org/10.1016/j.jocd.2018.09.003. (Epub ahead of print).

Cao, Y., Mori, S., Mashiba, T., Westmore, M.S., Ma, L., Sato, M., Akiyama, T., Shi, L., Komatsubara, S., Miyamoto, K., Norimatsu, H., 2002. Raloxifene, estrogen, and alendronate affect the process of fracture repair differently in ovariectomized rats. JBMR 17, 2237–2246.

Chen, G.X., Zheng, S., Qin, S., Zhong, Z.M., Wu, X.H., Huang, Z.P., Li, W., Ding, R.T., Yu, H., Chen, J.T., 2014. Effect of low-magnitude whole body vibration combined with alendronate in ovariectomized rats: a random controlled osteoporosis prevention study. PLoS One 9, e96181. https://doi.org/10.1371/journal.pone.0096181.

Chow, D.H.K., Leung, K.-S., Qin, L., Leung, A.H.-C., Cheung, W.-H., 2011. Low-magnitude high-frequency vibration (LMHFV) enhanced bone remodelling in osteoporotic rat femoral fracture healing. J. Orthop. Res. 29, 746–752.

Collins, B.C., Mader, T.L., Cabelka, C.A., Iñigo, M.R., Spangenburg, E.E., Lowe, D.A., 2018. Deletion of estrogen receptor alpha in skeletal muscle results in impaired contractility in female mice. J. Appl. Physiol. (1985). https://doi.org/10.1152/japplphysiol.00864.2017. 2018 Jan 18.

Dempster, D.W., Compston, J.E., Drezner, M.K., Glorieux, F.H., Kanis, J.A., Malluche, H., Meunier, P.J., Ott, S.M., Recker, R.R., Parfitt, A.M., 2012. Standardized nomenclature, symbols, and units for bone histomorphometry: a 2012 update of the report of the ASBMR histomorphometry nomenclature committee. JBMR 28, 1–16.

Fallon, J.B., Macefield, V.G., 2007. Vibration sensitivity of human muscle spindles and golgi tendon organs. Muscle Nerve 36, 21–29.

Faloona, G.R., Srere, P.A., 1969. Escherichia coli citrate synthase. Purification and the effect of potassium on some properties. Biochemistry 8, 4497–4503.

Ferretti, G., Fabi, A., Carlini, P., Papaldo, P., Cordiali Fei, P., Di Cosimo, S., Salesi, N., Giannarelli, D., Alimonti, A., Di Cocco, B., D'Agosto, G., Bordignon, V., Trento, E., Cognetti, F., 2005. Zoledronic-acid-induced circulating level modifications of angiogenic factors, metalloproteinases and proinflammatory cytokines in metastatic breast cancer patients. Oncology 69, 35–43.

Frost, H.M., 1997. On our age-related bone loss: insights from a new paradigm. JBMR 12, 1539–1546.

Gambacciani, M., Levancini, M., 2014. Hormone replacement therapy and the prevention of postmenopausal osteoporosis. Prz Menopauzalny 13, 213–220.

Giraudo, E., Inoue, M., Hanahan, D., 2004. An amino-bisphosphonate targets MMP-9-expressing macrophages and angiogenesis to impair cervical carcinogenesis. J. Clin. Invest. 114, 623–633.

Hatefi, Stiggall, D.L., 1978. Preparation and properties of NADH: cytochrome c oxidoreductase (complex I-III). Methods Enzymol. 53, 5–10.

Hernlund, E., Svedbom, A., Ivergård, M., Compston, J., Cooper, C., Stenmark, J., McCloskey, E.V., Jönsson, B., Kanis, J.A., 2013. Osteoporosis in the European Union: medical management, epidemiology and economic burden: a report prepared in collaboration with the International Osteoporosis Foundation (IOF) and the European Federation of Pharmaceutical Industry Associations (EFPIA). Arch. Osteoporos. 8 (1–2).

Hoffmann, D.B., Sehmisch, S., Hofmann, A.M., Eimer, C., Komrakova, M., Saul, D., Wassmann, M., Stürmer, K.M., Tezval, M., 2016a. Comparison of parathyroid hormone and strontium ranelate in combination with whole body vibration in a rat model of osteoporosis. J. Bone Miner. Metab. https://doi.org/10.1007/s00774-016-0736-0.

Hoffmann, D.B., Griesel, M.H., Brockhusen, B., Tezval, M., Komrakova, M., Menger, B., Wassmann, M., Stuermer, K.M., Sehmisch, S., 2016b. Effects of 8-prenylnaringenin and whole-body vibration therapy on a rat model of osteopenia. J. Nutr. Metab. 2016 (2016), 6893137. https://doi.org/10.1155/2016/6893137. (Epub 2016 Jan 19).

Hoppeler, H., 1986. Exercise-induced ultrastructural changes in skeletal muscle. Int. J. Sports Med. 7, 187–204.

Horak, V., 1983. A successive histochemical staining for succinate dehydrogenase and "reversed"—ATPase in a single section for the skeletal muscle fibre typing. Histochem. Cell Biol. 78, 545–553.

Hsu, W.L., Chen, C.Y., Tsauo, J.Y., Yang, R.S., 2014. Balance control in elderly people with osteoporosis. J. Formos. Med. Assoc. 113 (6), 334–339. https://doi.org/10.1016/j.jfma.2014.02.006.

Hümpel, M., Isaksson, P., Schaefer, O., Kaufmann, U., Ciana, P., Maggi, A., Schleuning, W.D., 2005a. Tissue specificity of 8-prenylnaringenin: protection from ovariectomy induced bone loss with minimal trophic effects on the uterus. J. Steroid Biochem. Mol. Biol. 97 (3), 299–305.

Hümpel, M., Schleuning, W.-D., Schaefer, O., Isaksson, P., Bohlmann, R., 2005b. Use of 8-Prenylnaringenin for Hormone Replacement Therapy. European Patent Application (Bulletin 2005/16 (EP 1 524 269 A1)). https://patentimages.storage.googleapis.com/52/e5/6f/f2743c9950bffa/EP1524269A1.pdf.

ISO, 1997. The International Organization for Standardization. Mechanical Vibration and Shock - Evaluation of Human Exposure to Whole-body Vibration. Part 1: General Requirements. vols. 2631-1 ISO, Geneva (28p).

Kalu, D.N., 1991. The ovariectomized rat model of postmenopausal bone loss. Bone Miner. 15, 175–192.

Karacan, I., Cidem, M., Cidem, M., Türker, K.S., 2017. Whole-body vibration induces distinct reflex patterns in human soleus muscle. J. Electromyogr. Kinesiol. 34, 93–101.

Keiler, A.M., Zierau, O., Kretzschmar, G., 2013. Hop extracts and hop substances in treatment of menopausal complaints. Planta Med. 79, 576–579.

Kolios, L., Hoerster, A.K., Sehmisch, S., Malcherek, M.C., Rack, T., Tezval, M., Seidlova-Wuttke, D., Wuttke, W., Stuermer, K.M., Stuermer, E.K., 2010. Do estrogen and alendronate improve metaphyseal fracture healing when applied as osteoporosis prophylaxis? Calcif. Tissue Int. 86, 23–32.

Komrakova, M., Werner, C., Wicke, M., Nguyen, B.T., Tezval, M., Semisch, S., Stuermer, K.M., Stuermer, E.K., 2009. Effect of daidzein, 4-methylbenzylidene camphor or estrogen on gastrocnemius muscle of osteoporotic rats undergoing tibia healing period. J. Endocrinol. 201, 253–262.

Komrakova, M., Krischek, C., Wicke, M., Sehmisch, S., Tezval, M., Rohrberg, M., Brandsch, T., Stuermer, K.M., Stuermer, E.K., 2011a. Influence of intermittent administration of parathyroid hormone on muscle tissue and bone healing in orchiectomized rats or controls. J. Endocrinol. 209, 9–19.

Komrakova, M., Sehmisch, S., Tezval, M., Schmelz, U., Frauendorf, H., Grueger, T., Wessling, T., Klein, C., Birth, M., Stuermer, K.M., Stuermer, E.K., 2011b. Impact of 4-methylbenzylidene camphor, daidzein, and estrogen on intact and osteotomized bone in osteopenic rats. J. Endocrinol. 211, 157–168.

Komrakova, M., Sehmisch, S., Tezval, M., Ammon, J., Lieberwirth, P., Sauerhoff, C., Trautmann, L., Wicke, M., Dullin, C., Stuermer, K.M., Stuermer, E.K., 2013. Identification of a vibration regime favorable for bone healing and muscle in estrogen-deficient rats. Calcif. Tissue Int. 92, 509–520.

Komrakova, M., Weidemann, A., Dullin, C., Ebert, J., Tezval, M., Stuermer, K.M., Sehmisch, S., 2015. The impact of strontium ranelate on metaphyseal bone healing in ovariectomized rats. Calcif. Tissue Int. https://doi.org/10.1007/s00223-015-0019-0.

Komrakova, M., Hoffmann, D.B., Nuehnen, V., Stueber, H., Wassmann, M., Wicke, M., Tezval, M., Stuermer, K.M., Sehmisch, S., 2016. The effect of vibration treatments combined with teriparatide or strontium ranelate on bone healing and muscle in ovariectomized rats. Calcif. Tissue Int. 99, 408–422.

Komrakova, M., Stuermer, E.K., Tezval, M., Stuermer, K.M., Dullin, C., Schmelz, U., Doell, C., Durkaya-Burchhard, N., Fuerst, B., Genotte, T., Sehmisch, S., 2017. Evaluation of twelve vibration regimes applied to improve spine properties in ovariectomized rats. Bone Rep. 7, 172–180.

Komrakova, M., Fiebig, J., Hoffmann, D.B., Krischek, C., Lehmann, W., Stuermer, K.M., Sehmisch, S., 2018. The advantages of bilateral osteotomy over unilateral osteotomy for osteoporotic bone healing. Calcif. Tissue Int. 3, 80–94.

Kyriakides, Z.S., Petinakis, P., Kaklamanis, L., Sbarouni, E., Karayannakos, P., Iliopoulos, D., Dontas, I., Kremastinos, D.T., 2001. Intramuscular administration of estrogen may promote angiogenesis and perfusion in a rabbit model of chronic limb ischemia. Cardiovasc. Res. 49, 626–633.

Lei, Z., Xiaoying, Z., Xingguo, L., 2009. Ovariectomy-associated changes in bone mineral density and bone marrow haematopoiesis in rats. Int. J. Exp. Pathol. 90, 512–519.

Livak, K.J., Schmittgen, T.D., 2001. Analysis of relative gene expression data using real-time quantitative PCR and the 2-DDCT method. Methods 25, 402–408.

Luo, D., Kang, L., Ma, Y., Chen, H., Kuang, H., Huang, Q., He, M., Peng, W., 2014. Effects and mechanisms of 8-prenylnaringenin on osteoblast MC3T3-E1 and osteoclast-like cells RAW264.7. Food Sci. Nutr. 2, 341–350.

Lynch, M.A., Brodt, M.D., Stephens, A.L., Civitelli, R., Silva, M.J., 2011. Low-magnitude whole-body vibration does not enhance the anabolic skeletal effects of intermittent PTH in adult mice. J. Orthop. Res. 29, 465–472. https://doi.org/10.1002/jor.21280.

Maddalozzo, G.F., Iwaniec, U.T., Turner, R.T., Rosen, C.J., Widrick, J.J., 2008. Whole-body vibration slows the acquisition of fat in mature female rats. Int. J. Obes. 32, 1348–1354.

Milligan, S., Kalita, J., Pocock, V., Heyerick, A., De Cooman, L., Rong, H., De Keukeleire, D., 2002. Oestrogenic activity of the hop phyto-oestrogen, 8-prenylnaringenin. Reproduction 123, 235–242.

Miyamoto, M., Matsushita, Y., Kiyokawa, A., Fukuda, C., Iijima, Y., Sugano, M., Akiyama, T., 1998. Prenylflavonoids: a new class of non-steroidal phytoestrogen (part 2). Estrogenic effects of 8-isopentenylnaringenin on bone metabolism. Planta Med. 64, 516–519.

Mukai, R., Horikawa, H., Fujikura, Y., Kawamura, T., Nemoto, H., Nikawa, T., Terao, J., 2012. Prevention of disuse muscle atrophy by dietary ingestion of 8-prenylnaringenin in denervated mice. PLoS One 7 (9), e45048. https://doi.org/10.1371/journal.pone.0045048. 2012. (Epub 2012 Sep 19).

Namkung-Matthai, H., Appleyard, R., Jansen, J., Hao Lin, J., Maastricht, S., Swain, M., Mason, R.S., Murrell, G.A., Diwan, A.D., Diamond, T., 2001. Osteoporosis influences the early period of fracture healing in a rat osteoporotic model. Bone 28, 80–86.

Orwoll, E., Ettinger, M., Weiss, S., Miller, P., Kendler, D., Graham, J., Adami, S., Weber, K., Lorenc, R., Pietschmann, P., Vandormael, K., Lombardi, A., 2000. Alendronate for the treatment of osteoporosis in men. N. Engl. J. Med. 343, 604–610.

Oxlund, B.S., Ørtoft, G., Andreassen, T.T., Oxlund, H., 2003. Low intensity, high-frequency vibration appears to prevent the decrease in strength of the femur and tibia associated with ovariectomy of adult rats. Bone 32, 69–77.

Petcu, E.B., Ivanovski, S., Wright, R.G., Slevin, M., Miroiu, R.I., Brinzaniuc, K., 2012. Bisphosphonate-related osteonecrosis of jaw (BRONJ): an anti-angiogenic side-effect? Diagn. Pathol. 7, 78.

Peter, J.B., Barnard, R.J., Edgerton, V.R., Gillespie, C.A., Stempel, K.E., 1972. Metabolic profiles of the three fiber types of skeletal muscle in Guinea pigs and rabbits. Biochemistry 11, 2627–2633.

Rolland, Y., Czerwinski, S., Van Kan, G.A., Morley, J.E., Cesari, M., Onder, G., Woo, J., Baumgartner, R., Pillard, F., Boirie, Y., Chumlea, W.M., Vellas, B., 2008. Sarcopenia: its assessment, etiology, pathogenesis, consequences and future perspectives. J. Nutr. Health Aging 12, 433–450.

Rosalski, S.B., 1998. Low serum creatine kinase activity. Clin. Chem. 44, 905.

Rubinacci, A., Marenzana, M., Cavani, F., Colasante, F., Villa, I., Willnecker, J., Moro, G.L., Spreafico, L.P., Ferretti, M., Guidobono, F., Marotti, G., 2008. Ovariectomy sensitizes rat cortical bone to whole-body vibration. Calcif. Tissue Int. 82, 316–326.

Rueff-Barroso, C.R., Milagres, D., do Valle, J., Casimiro-Lopes, G., Nogueira-Neto, J.F., Zanier, J.F., et al., 2008. Bone healing in rats submitted to weight-bearing and non-weight-bearing exercises. Med. Sci. Monit. 14, BR231–236.

Sehmisch, S., Hammer, F., Christoffel, J., Seidlova-Wuttke, D., Tezval, M., Wuttke, W., Stuermer, K.M., Stuermer, E.K., 2008. Comparison of the phytohormones genistein, resveratrol and 8-prenylnaringenin as agents for preventing osteoporosis. Planta Med. 74, 794–801.

Shapses, S.A., Riedt, C.S., 2006. Bone, body weight, and weight reduction: what are the concerns? J. Nutr. 136, 1453–1456.

Slatkovska, L., Alibhai, S.M.H., Beyene, J., Cheund, A.M., 2010. Effect of whole-body vibration on BMD: a systematic review and metaanalysis. Osteoporos. Int. 21, 1969–1980.

Stuermer, E.K., Sehmisch, S., Rack, T., Wenda, E., Seidlova-Wuttke, D., Tezval, M., Wuttke, W., Frosch, K.H., Stuermer, K.M., 2010. Estrogen and raloxifene improve metaphyseal fracture healing in the early phase of osteoporosis. A new fracture-healing model at the tibia in rat. Langenbeck's Arch. Surg. 395, 163–172.

Stuermer, E.K., Komrakova, M., Sehmisch, S., Tezval, M., Dullin, C., Schaefer, N., Hallecker, J., Stuermer, K.M., 2014. Whole body vibration during fracture healing intensifies the effects of estradiol and raloxifene in estrogen-deficient rats. Bone 64, 187–194.

Štulíková, K., Karabín, M., Nešpor, J., Dostálek, P., 2018. Therapeutic perspectives of 8-prenylnaringenin, a potent phytoestrogen from hops. Molecules 23, 660.

Tienboon, P., Jaruwangsanti, N., 2014. A prospective analytical study of the effects and adverse events of alendronate (Aldren70) treatment in Thai postmenopausal women. J. Med. Assoc. Thail. 97, 621–628.

Toth, M.J., Poehlman, E.T., Matthews, D.E., Tchernof, A., MacCoss, M.J., 2001. Effects of estradiol and progesterone on body composition, protein synthesis, and lipoprotein lipase in rats. Am. J. Physiol. Endocrinol. Metab. 280, E496–E501.

Turner, R.T., Riggs, B.L., Spelsberg, T.C., 1994. Skeletal effects of estrogen. Endocr. Rev. 15, 275–300.

Uchiyama, S., Ikegami, S., Kamimura, M., Mukaiyama, K., Nakamura, Y., Nonaka, K., Kato, H., 2015. The skeletal muscle cross sectional area in long-term bisphosphonate users is smaller than that of bone mineral density-matched controls with increased serum pentosidine concentrations. Bone 75, 84–87. https://doi.org/10.1016/j.bone.2015.02.018.

Valberg, S.J., 2008. Clinical biochemistry of domestic animals. In: Chapter 15 - Skeletal Muscle Function, Sixth edition. Copyright © 2008 Elsevier Inc., pp. 459–484. https://doi.org/10.1016/B978-0-12-370491-7.00015-5.

Verschueren, S.M.P., Roelants, M., Delecluse, C., Swinnen, S., Vanderschueren Boonen, S., 2004. Effect of 6-month whole body vibration training on hip density, muscle strength, and postural control in postmenopausal women: a randomized controlled pilot study. J. Bone Miner. Res. 19, 352–359.

Wang, J., Leung, K.S., Chow, S.K., Cheung, W.H., 2017. The effect of whole body vibration on fracture healing - a systematic review. Eur. Cell. Mater. 34, 108–127.

Wehrle, E., Liedert, A., Heilmann, A., Wehner, T., Bindl, R., Fischer, L., Haffner-Luntzer, M., Jakob, F., Schinke, T., Amling, M., Ignatius, A., 2015a. The impact of low-magnitude high-frequency vibration on fracture healing is profoundly influenced by the oestrogen status in mice. Dis. Model. Mech. 8, 93–104. https://doi.org/10.1242/dmm.018622.

Wehrle, E., Liedert, A., Heilmann, A., Wehner, T., Bindl, R., Fischer, L., Haffner-Luntzer, M., Jakob, F., Schinke, T., Amling, M., Ignatius, A., 2015b. The impact of low-magnitude high frequency vibration on fracture healing is profoundly influenced by the oestrogen status in mice. Dis. Model. Mech. 8, 93–104.

Widrick, J.J., Fuchs, R., Maddalozzo, G.F., Marley, K., Snow, C., 2007. Relative effects of exercise training and alendronate treatment on skeletal muscle function of ovariectomized rats. Menopause 14 (3 Pt 1), 528–534.

Wiik, A., 2008. Estrogen Receptors in Skeletal Muscle - Expression and Activation. (Diss. Ph.D. Stockholm).

Wolfe, R.R., 2006. The underappreciated role of muscle in health and disease. Am. J. Clin. Nutr. 84 (3), 475–482.

Wysocki, A., Butler, M., Shamliyan, T., Kane, R.L., 2011. Whole-body vibration therapy for osteoporosis: state of the science. Ann. Intern. Med. 155, 680–686.

Xie, L., Rubin, C., Judex, S., 2008. Enhancement of the adolescent murine musculoskeletal system using low-level mechanical vibrations. J. Appl. Physiol. 104, 1056–1062. https://doi.org/10.1152/japplphysiol.00764.2007.

Yingjie, H., Ge, Z., Yisheng, W., Ling, Q., Hung, W.Y., Kwoksui, L., Fuxing, P., 2007. Changes of microstructure and mineralized tissue in the middle and late phase of osteoporotic fracture healing in rats. Bone 41, 631–638.

Zhou, W., Slingerland, J.M., 2014. Links between oestrogen receptor activation and proteolysis: relevance to hormoneregulated cancer therapy. Nat. Rev. Cancer 14, 26–38.